

Nomenclature:

List of variables:

- HSC High strength concrete
- FRC Fibre-reinforced concrete
- HPC High performance concrete
- SCMs Supplementary cementing materials
- IS Indian standards
- SSA Specific surface area
- LOI Loss on ignition

- ASTM American Society for Testing and Materials
- CS Compressive strength
- MoE Modulus of elasticity
- SEM Dimensionless temperature

Greek Symbols:

- G Specific gravity
- μ Particle size in micrometer ($X \times 10^{-6}$)

Nanotechnology is a multidisciplinary science and engineering subject concerned with understanding and directing materials with dimensions ranging from one to one hundred nanometers. Nanomaterials are employed in a variety of unique applications such as agriculture, medical, electronics, infrastructure, food, fuels, air and water cleaners, chemical sensors, fabric, and so on. Depending on the nanomaterial dimensions, they can be separated into four different groups, namely called Zero-dimensional (0D), One-dimensional (1D), Two-dimensional (2D) and Three-dimensional (3D). A recent and interesting area of research is the incorporation of nanoparticles in concrete matrix. To enhance the characteristics of concrete, several nanomaterials have recently been used. Nanomaterial uses have a higher potential to diminish the environmental impact of energy intensity and enhance the structure’s lifespan. Hence, the research on nanomaterials in concrete is crucial to making concrete more environmentally friendly. It is crucial to study nanomaterials’ application to improve cement-based composites’ properties. Still, only a few studies are available on nanomaterial use in ultra-high-performance concrete. Over the past two decades, the growing application of nano Al₂O₃ particles as SCM only in cement paste, mortar, shotcrete, normal strength concrete, and high strength concrete has been widely investigated. Now, there are only a few studies are available on the use of nanomaterials in UHPC. Blending nanomaterials in UHPC would be a breakthrough in the vision for future sustainability needs, creating extraordinary applications in the construction sector. The proposed research will cover a knowledge gap in the impacts of nano Al₂O₃ particle substitution on the slump cone, strength test, modulus of elasticity, water permeability and microstructural properties features of UHPC.

2. Materials

In the current study, OPC53 grade cement was used in accordance with IS: 12269-2013 [32]. The river sand is used as fine aggregate and has a specific gravity of 2.64, bulk density of 1650kg/m³ and water absorption of 0.55%, respectively, according to IS 2386–Part 1 [33]. Elkem Microsilica® 940 type densified silica fume obtained from Elkem Metallurgy (P) Ltd is utilized, which conforms to IS 15388: 2003 [34]. Figure 1 depicts the morphology, elemental content, and particle size distribution of silica fume as described in Table 1.

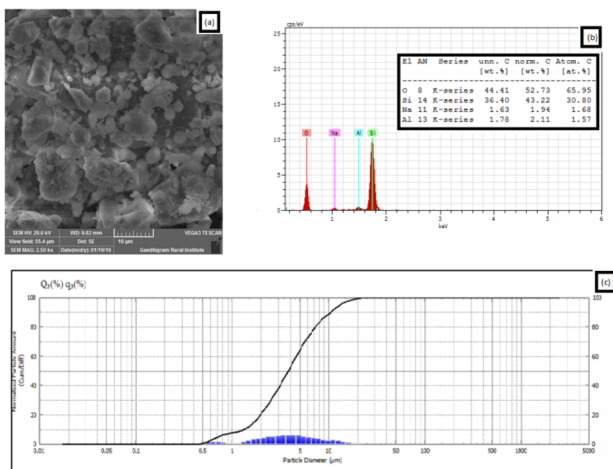


Figure 1. The characterization silica fume.

Nano-Al₂O₃ particles with a SSA of 180 m²/g is used in this study. Table 2 illustrates the properties of the nano-Al₂O₃ particles and their appearance, elemental composition and XRD spectra in Fig. 2.

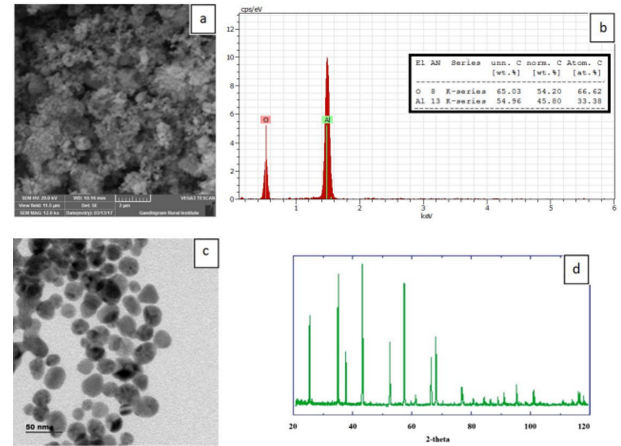


Figure 2. The characterization of nano-Al₂O₃ particles (a) SEM, (b) EDAX elemental composition and (c) TEM and (d) XRD.

Table 1. The properties of the silica fume.

An example of a column heading	Property	Values
Chemical Properties	Moisture Content	00.63%
	SiO ₂	96.12%
	LOI	02.42%
Physical Properties	Specific Gravity	02.31
	Visibility	Grayish Powder
	State	Amorphous
	Bulk Density	700 (kg/m ³)
	SSA	23.18 (m ² /g)
	Solubility	Insoluble

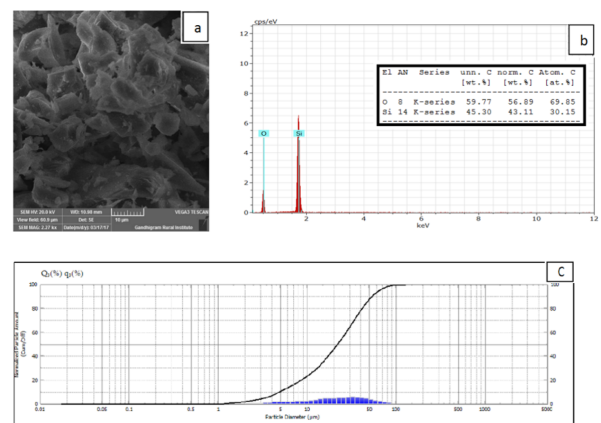


Figure 3. The categorization of quartz powder.

The quartz powder that was obtained from Gayathiri Enterprise (P) Ltd. has an average particle size of 19 μm. The manufacturer’s disclosure of the quartz powder’s physical and chemical characteristics is displayed in Table 3. Also, the Fig. 3 displays the powder’s morphology, elemental content, and particle size distribution curve. The Polypropylene fiber procured from the Fibre zone Company is used, conforming to BS EN 14889-2: 2006 [35]. The physical

properties are presented in Table 4. The Auramix 400, a modified polycarboxylic ether-based new generation superplasticizer is utilized and its properties are presented in Table 5. Potable drinking water accessible in the laboratory is used for conforming to IS 456-2000 [36], which is used for the casting and curing of specimens.

Table 2. The physical and chemical properties of the nanoparticle (quartz powder) of Aluminum Oxide.

Density (g/cm^3)	Purity (%)	Size (nm)	SSA (m^2/g)	Morphology	MW	Color
3.7	99.99	20-30	180	Spherical	101.96	White powder

Table 3. The properties of the quartz powder.

Grades	SiO_2	Al_2O_3	Fe_2O_3	Boiling Point	Specific Gravity	State
300 MESH	99.6%	0.1%	0.01%	Above 1300C°	2.65	White powder

Table 4. The polypropylene fiber physical properties.

Colour	White
Density (g/cm^3)	0.91
Burning Point, C°	> 360
Melting point, C°	160-180
Fiber diameter, μm	38
Acid resistance	Fine
Tensile Strength, (MPa)	> 500
Elongation rate	> 15%

Table 5. The properties of superplasticizers.

Superplasticizer type	ASTM C494 Type F
PH	> 6
Aspect	Reddish brown liquid
Chloride ion content	< 0.2%
Relative Density	1.08 at 25 C°

3. Mix proportions

There is a lack of design code for the mix design of UHPC, so the mix UHPC mix is optimized according to the literature and prepared as per the requirement of ASTM C1856 [37]. Based on the laboratory trails, the totally seven UHPC mixtures are optimized and shown in Table 6. The water to binder ratio is fixed at 0.24 continuously for all mixes. Seven types of UHPC mixtures are divided into two series, each with a different dosage of cement and nanoparticles while always totalizing low cement content of $570.45 kg/m^3$. These include one-control mixtures (CON mix -without nanoparticles), and the other six mixtures are produced with different dosage levels of nano Al₂O₃ particles 0.5% to 3% replacement with an increment of 0.5%, respectively. The content of polypropylene (PP) fibers amount is added by 0.4% to the volume of concrete. Silica fume, Quartz powder and sand content water were fixed in all mixes at $171.20 kg/m^3$, $245.28 kg/m^3$ and $1245.38 kg/m^3$, respectively, respectively. All seven mixtures are prepared in a mortar mixer with a total mixing time of 30 minutes. Furthermore, mixing is always done in a laboratory environment using dried, tempered aggregates and powder components. The room temperature is 24C° for mixing, testing, and concreting. The mixing, casting and curing procedure are adopted as summarized below:

- The nano Al₂O₃ particles are dispersed in 20% PCE and 20% water using a bath sonication technique for 30 min.
- Cement, quartz powder, sand, and Silica fume are placed in a mortar mixer and mixed slowly for 5 min.
- 60% of PCE is mixed with 80% water are added slowly to the dry mixture. The mixing continues up to granules' transformation (about 10 min).

- After forming the granules, the dispersed nano Al₂O₃ particles mix is added slowly and mixing is continued for another 5 min. Subsequently, the remaining 20% of the PCE is added to the mixture and mixed for 5 min at high speed until the transformation of the mixture into a homogenous mix.
- Then polypropylene fibers are added to the mixture slowly and mixed for 5 min. After that, the mixing is continued for a further period of 5 min to well dispersion of the UHPC mixture.
- The produced UHPC mixture is partially taken for fresh concrete tests. The remaining concrete is filled with moulds, with the plastic sheets covering the surface and kept for 24 hours at laboratory temperature.
- After that the demoulded specimens are placed in normal water curing at room temperature.

4. Testing of Concrete

4.1 Mini slump flow

The flow of fresh concrete mix is measured by mini-slump cone according to the ASTM C1437-07 [38]. The freshly prepared concrete mix is placed into the mini slump cone having bottom diameter 100 mm and a top diameter of 70 mm and height 50 mm. The concrete mix is filled with a single layer without compaction, which is specified by ASTM 1856/C1856-17 [39]. Then the cone is lifted slowly which allows the concrete to flow. The largest width of concrete spread is noted as d1 and then the d2 is measured by right angles to d1.

4.2 Compressive strength

The compressive strength of specimens is tested as per the IS: 516-1959 [40] at the age of 1, 3, 7, 14, 28 and 56 days of curing. The saturated surface dried 50mm cube specimens are tested in 3000KN AMIL digital compression testing machine at a rate of 900 N/s.

4.3 Modulus of elasticity

As per ASTM C 469 – 02 [41], the static modulus of elasticity of concrete is measured by using of deflection gauge method in cylindrical specimens having a size of 100 mm diameter and 200 mm height at the age of 28 and 56 days. In this method of testing, the specimen is placed between the loading plates of digital CTM and the dial gauge is fixed on both sides of the bottom plate. Then apply the axial load continuously without shock at constant rate 0.25 N/mm². The deflection gauge is used to record the length changes of the specimens which is used for the axial strain measurement of specimens.

4.4 Water permeability

The depth to which water may penetrate specimens (100mm cubes) under pressure is determined after 28 and 56 days using a water permeability device, following the guidelines provided in BSEN 12390-8:2009 [42]. Apply a water pressure of 500 kPa for a duration of 72 hours, and thereafter remove the specimen from the device. Clean the surface where water pressure is exerted to eliminate any remaining water. Divide the specimen into two equal halves at a right angle to the surface where the water pressure is exerted. Determine the greatest extent of penetration under the designated region and document using a Vernier calliper. The greatest depth of penetration, measured in millimetres.

4.5 Micro-structural Properties

The broken concrete samples after compression testing are collected and performed SEM.

5. Results and Discussion

5.1 The Mini Slump Test

The mini-slump flow was tested according to the ASTM C1437-07 [38]. The Table 6 listed the flow properties of UHPC with and without nano Al₂O₃ particles. It shows that the lowest slump flow spread of 240 mm is observed in the control mix without nano Al₂O₃ particles, and for the nano Al₂O₃ admixed mixes the slump value ranges from 242mm to 251 mm. From the results, it is understood that the inclusion of nano Al₂O₃ particles has improved the flow of mix without adjusting the superplasticizer dosage. However, 3% of nano Al₂O₃ particles added to mix is reached largest spread of 251 mm, which increased flow by 3.33%, in comparison to the control mix. Kazempour et al. 2015 [43] and Khorasani et al. 2015 [44] reported that the higher dosage of nano alumina are decreased the flow of mortar, due to increasing the cohesiveness of the

Table 6. The mix proportions.

Mix ID	Cement (kg/m^3)	Nano Al ₂ O ₃ (kg/m^3)	Silicafume (kg/m^3)	Sand (kg/m^3)	QP (kg/m^3)	Water (kg/m^3)	PCE (kg/m^3)	PP Vol. (%)
CON	570.45	00.00	171.20	1245.38	245.28	178	22.818	0.4
0.5AL	567.60	02.85	171.20	1245.38	245.28	178	22.818	0.4
1.0AL	564.75	05.70	171.20	1245.38	245.28	178	22.818	0.4
1.5AL	561.89	08.56	171.20	1245.38	245.28	178	22.818	0.4
2.0AL	559.04	11.41	171.20	1245.38	245.28	178	22.818	0.4
2.5AL	556.19	14.26	171.20	1245.38	245.28	178	22.818	0.4
3.0AL	553.33	17.12	171.20	1245.38	245.28	178	22.818	0.4

mixtures. When the nano alumina particles were directly added in mix without dispersing, it has increased the yield stress and viscosity of mortar, due to their high reactivity and surface area. Nazari and Riahi (2011a; b) [45, 46] has reported that the nano alumina particles blended concrete mixtures have low slump values, the cement substitute with nano alumina particles will increase the water demand due to the increase in surface area. But in this study, the addition of nano Al₂O₃ particles has increased the fluidity of the mix and become more workable and easier to placement, in all nano Al₂O₃ particles blended mixtures. This may due to the well dispersion of nano Al₂O₃ particles has reduced the yield stress and viscosity of the mix, which leads to enhance the workability of the fresh concrete.

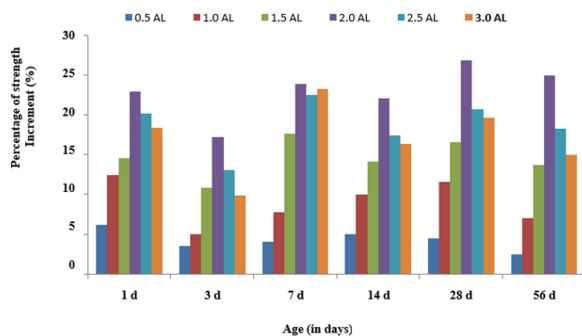


Figure 4. The percentage of enhancement in compressive strength.

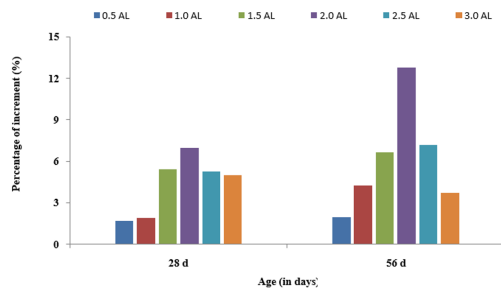


Figure 5. The percentage of enhancement in modulus of elasticity.

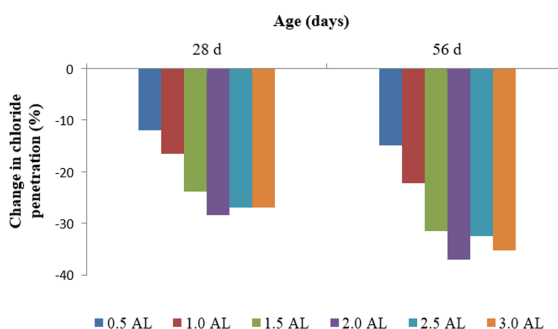


Figure 6. The percentage of reduction in water penetration of depth under pressure.

5.2 Compressive Strength (CS)

The CS of specimens was tested as per ASTM C109/C10M – 07 [47] at the different ages of curing. The effect of nano Al₂O₃ particles replacement on the compressive strength and percentage of strength enhancement are depicted in Fig. 4. It could be seen that the minimum CS noticed in the control mix was 55.05 MPa, 71.28 MPa, 91.41 MPa, 103.32 MPa, 122.65 MPa and 129.57 MPa at the age of 1, 3, 7, 14, 28, and 56 days respectively. However, the CS of UHPC is increased with every case of nano Al₂O₃ particles replacement percentage and it has higher than the control mix strength. Whereas, the highest CS observed in 2.0 AL mix was 67.65 MPa, 83.57 MPa, 113.28 MPa, 126.13 MPa, 155.59 MPa and 161.92 MPa at an age of 1, 3, 7, 14, 28 and 56 days respectively. The 2% of Al₂O₃ particles replacement is found as optimum level for efficiency and economical point of view, which has increased CS by 22.89%, 17.24%, 23.93%, 22.09%, 26.86% and 24.97% at 1, 3, 7, 14, 28, and 56 days respectively in comparison to control mix. This strength improvement is mainly attributed due to the filler effect and pozzolanic reactivity of nano Al₂O₃ particles. The nano Al₂O₃ particles acts as a dynamic reactive substance in the arrangement of nuclei cite during C-S-H gel formation as well as it's promoting hydration process, which leads to refined pores and densifies the microstructure. In addition, the nano Al₂O₃ particle has reduced the distance between cement grains and SCM particles, which makes the cement matrix as more homogenous and compact microstructure. As a result, it enhanced the CS rapidly at early ages and later it increased gradually with curing days.

5.3 Modulus of Elasticity (MOE)

The MOE test was performed in accordance to ASTM C 469 – 02. The influence of nano Al₂O₃ particle replacement on the MOE of UHPC mixes is depicted in Fig. 5. It is observed that the modulus of elasticity is increased with nano Al₂O₃ particles content up to 2% and beyond that dosage, it has decreased the MOE but those values still higher than the control mix. The maximum modulus of elasticity value of 38.98 GPa is observed for 2.0 AL mix and the minimum of 36.43 GPa for the control mix at 28 days. Similarly for 56 days, the minimum and maximum modulus of elasticity achieved by control mix and 2.0 AL mix, which is 38.29 GPa and 43.19 GPa respectively. The 2% of Al₂O₃ particles were enhanced the modulus of elasticity by 7.00% and 12.80% at 28 and 56 days. The compressive strength and porosity of specimens play the vital role on the modulus of elasticity of concrete. The nano Al₂O₃ particles inclusion has enhanced the compressive strength of concrete and reduced the voids of UHPC. Furthermore, the nano Al₂O₃ particles has arrests cracks and restrict the continuity of slip plans which lead to improve the toughness of cement matrix. This might reason for increasing of modulus of elasticity of UHPC samples.

5.4 The water permeability

The water infiltration depth under pressure of UHPC mixes was examined conferring to the standards outlined in BS EN 12390-8:2009. Figure 6 shows the impact of substituting nano Al₂O₃ particles on the water penetration depth in UHPC samples after 28 and 56 days. after 28 days, the control mix showed a maximum water penetration depth of 1.34 mm, which decreased to 1.08 mm after 56 days. On the 2.0 AL mix, the minimal depth of water penetration was described to be 0.96 mm at 28 days and 0.68 mm at 56 days. The minimum water permeability is observed in the 2.0 AL mix is represented the less amount permeable voids in the mix, which is due to the filler effect of nano Al₂O₃ particles. Similar to the water absorption results, the inclusion of nano Al₂O₃ particles has reduced the volume of permeable voids in UHPC, which has reduced of the water penetration depth at all ages. Similar results were found in the previous research work of Arefi et al. 2011 [48].

5.5 SEM analysis

The samples are collected after the testing compressive strength of concrete and immersed in anhydrous ethanol to stop further hydration process. These

samples are utilized for studying micro-structural analysis by SEM test. The microscopic images of UHPC surface is captured at an age of 3, 14, and 28 days as per the ASTM C1723–16 [49]. Figure 7 displays SEM images of the CON mix and 2.0 AL mix, taken on the 28th day. The micrographs in Fig. 7a and b clearly demonstrate the presence of a significant number of micro pores in the cement matrix. The micrographs in Fig. 7c and d show that a homogeneous densified microstructure is found in the cement matrix of the 2.0 AL mix specimens. The sample containing 2% nano Al₂O₃ particles exhibits a denser micro-structure, with fewer spaces being filled by the nano Al₂O₃ particles. This is attributed to the quick processing of the C-S-H gel. The Ca(OH)₂ crystals have been reduced and transformed into more densely packed hydration products. The acquired results are consistent with those published by other studies.

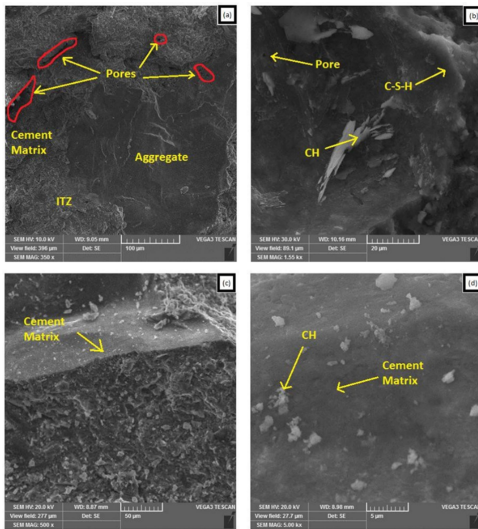


Figure 7. The SEM micrographs (a) & (b) CON mix, (c) & (d) 2.0 AL mix

6. Conclusions

The results are confirmed that the inclusion of nano Al₂O₃ particles is improved workability properties of the fresh UHPC and following results are observed while compared with control concrete without nano Al₂O₃ particles. 3% of nano Al₂O₃ particles is found optimum for enhancement of workability. The inclusion of 2% of nano Al₂O₃ particles were improved the mechanical properties of UHPC and following conclusion are drawn control concrete without nano Al₂O₃ particles. The compressive strength enhanced up to 26.86%. The modulus of elasticity enhanced by 7%. The SEM micrographs reveal the increase of nano Al₂O₃ particles were led to increase the hydration process and acts as a nucleation sites of CSH gel formation and pore-filling material in a cement matrix, therefore densified microstructure was produced compared to the control concrete. Also, the Ca(OH)₂ crystals were declined and a compact development of hydration products was perceived by exploiting this micrograph. The inclusion of 2% of nano Al₂O₃ particles were found as optimum percentage for durability enhancement. The water penetration depth, under pressure and sorptivity is reduced up to 37.04% and 15.34%, respectively.

Authors' contribution

S. Hariprasad Reddy: conceptualization of research, drafting the research manuscript, reviewing, editing, and preparation of the final draft. K. Mahaboob Peera: Data collection, manuscript review, and editing. A. Surendra, C. Arvind Kumar, M. Leelakar: contributed to various aspects of the research work as needed.

Declaration of competing interest

The authors declare no conflicts of interest.

Funding source

This study didn't receive any specific funds.

Data availability

The data and images used in this study were collected and processed directly by the researchers as primary research materials. Requests for data sharing can be fulfilled upon reasonable inquiry to the research team.

Acknowledgements

The authors extend their gratitude to the Department of Civil Engineering at Srinivasa Ramanujan Institute of Technology, Ananthapuramu, India, for generously providing access to their laboratory testing facilities.

REFERENCES

- [1] Y. Shi, G. Long, X. Zen, Y. Xie, and T. Shang, "Design of binder system of eco-efficient uhpc based on physical packing and chemical effect optimization," *Construction and Building Materials*, vol. 274, p. 121382, 2021. [Online]. Available: <https://doi.org/10.1016/j.conbuildmat.2020.121382>
- [2] C. Gu, G. Ye, and W. Sun, "Ultrahigh performance concrete-properties, applications and perspectives," *Sci. China Technol. Sci.*, vol. 58, no. 4, p. 587–599, 2015. [Online]. Available: <https://doi.org/10.1007/s11431-015-5769-4>
- [3] A. Zeyad, I. Hakeem, M. Amin, B. Tayeh, and I. Agwa, "Effect of aggregate and fibre types on ultra-high-performance concrete designed for radiation shielding," *J. Build. Eng.*, vol. 58, no. 2, p. 104960, 2022. [Online]. Available: <http://doi.org/10.1016/j.job.2022.104960>
- [4] M. Amin, I. Hakeem, A. Zeyad, B. Tayeh, A. Maglad, and I. Agwa, "Influence of recycled aggregates and carbon nanofibres on properties of ultra-high-performance concrete under elevated temperatures," *Case Stud. Constr. Mater.*, vol. 16, no. 12, p. e01063, 2022. [Online]. Available: <https://doi.org/10.1016/j.cscm.2022.e01063>
- [5] A. Karimipour, M. Ghalehnovi, J. de Brito, and M. Attari, "The effect of polypropylene fibres on the compressive strength, impact and heat resistance of self-compacting concrete," *Structures*, vol. 25, p. 72–87, 2020. [Online]. Available: <https://doi.org/10.1016/j.istruc.2020.02.022>
- [6] J. Wang, Q. Dai, R. Si, Y. Ma, and S. Guo, "Fresh and mechanical performance and freeze-thaw durability of steel fiber-reinforced rubber self-compacting concrete (srsc)," *Journal of Cleaner Production*, vol. 277, no. 1, p. 123180, 2020. [Online]. Available: <http://doi.org/10.1016/j.jclepro.2020.123180>
- [7] M. Amin, B. Tayeh, and I. Agwa, "Effect of using mineral admixtures and ceramic wastes as coarse aggregates on properties of ultrahigh-performance concrete," *J. Cleaner Production*, vol. 273, no. 4, p. 123073, 2020. [Online]. Available: <https://doi.org/10.1016/j.jclepro.2020.123073>
- [8] R. Choudhary, R. Gupta, and R. Nagar, "Impact on fresh, mechanical, and microstructural properties of high strength self-compacting concrete by marble cutting slurry waste, fly ash, and silica fume," *Constr. Build. Mater.*, vol. 239, no. 239c, p. 117888, 2019. [Online]. Available: <http://doi.org/10.1016/j.conbuildmat.2019.117888>
- [9] L. Gemi, E. Madenci, Y. Ozkicil, S. Yazman, and A. Safonov, "Effect of fiber wrapping on bending behavior of reinforced concrete filled pultruded gfrp composite hybrid beams," *Polymers*, vol. 14, no. 18, p. 3740, 2022. [Online]. Available: <https://doi.org/10.3390/polym14183740>
- [10] Y. Ozkılıç, C. Aksoyulu, Şakir yazman, L. Gemi, and M. Arslan, "Behavior of cfrp-strengthened rc beams with circular web openings in shear zones: Numerical study," *Structures, Elsevier*, vol. 41, no. 1, p. 1369–1389, 2022. [Online]. Available: <https://doi.org/10.1016/j.istruc.2022.05.061>
- [11] L. Gemi, M. Alsdudi, C. Aksoyulu, Şakir Yazman, and Y. O. Özk., "Optimum amount of cfrp for strengthening shear deficient reinforced concrete beams," *Steel and Composite Structures*, vol. 43, no. 6, p. 735–757, June 2022. [Online]. Available: <http://doi.org/10.12989/scs.2022.43.6.735>
- [12] A. Rashno and A. Saghaeifar, "Durability of ultra-high-performance self-compacting concrete with hybrid fibers," *Emerging Materials Research*, vol. 9, no. 2, pp. 331–341, 2020. [Online]. Available: <https://doi.org/10.1680/jemmr.19.00083>
- [13] J. Haido, B. Tayeh, S. Alhushkizi, and M. Karpuzcu, "Effect of high temperature on the mechanical properties of basalt fibre self-compacting concrete as an overlay material," *Constr. Build. Mater.*, vol. 268, no. 1, p. 121725, 2020. [Online]. Available: <http://doi.org/10.1016/j.conbuildmat.2020.121725>
- [14] X. Yu, B. Zhou, F. Hu, Y. Zhang, X. Xu, C. Fan, W. Zhang, H. Jiang, and P. Liu, "Experimental investigation of basalt fiber-reinforced polymer (bfrp) bar reinforced concrete slabs under contact explosions," *Int. J. Impact Eng.*, vol. 144, no. 4, p. 103632, 2020. [Online]. Available: <http://doi.org/10.1016/j.ijimpeng.2020.103632>
- [15] M. Li, F. Gong, and Z. Wu, "Study on mechanical properties of alkali-resistant basalt fiber reinforced concrete," *Constr. Build. Mater.*, vol. 245, p. 118424, 2020. [Online]. Available: <http://doi.org/10.1016/j.conbuildmat.2020.118424>

- [16] W. Yonggui, L. Shuai-peng, P. Hughes, and F. Yuhui, "Mechanical properties and microstructure of basalt fibre and nano-silica reinforced recycled concrete after exposure to elevated temperatures," *Constr. Build. Mater.*, vol. 247, no. 1, p. 118561, June 2020. [Online]. Available: <https://doi.org/10.1016/j.conbuildmat.2020.118561>
- [17] M. Karalar, Y. Ozkılıç, A. Deifalla, C. Aksoylu, M. Arslan, M. Ahmad, and M. Sabri, "Improvement in bending performance of reinforced concrete beams produced with waste lathe scraps," *Sustainability*, vol. 14, no. 19, p. 12660, 2022. [Online]. Available: <https://doi.org/10.3390/su141912660>
- [18] A. Çelik, Y. Ozkılıç, O. Zeybek, N. Öner, and B. Tayeh, "Performance assessment of fiber-reinforced concrete produced with waste lathe fibers," *Sustainability*, vol. 14, no. 19, p. 11817, September 2022. [Online]. Available: <https://doi.org/10.3390/su141911817>
- [19] C. Aksoylu, Y. Ozkılıç, M. Hadzima-Nyarko, E. I. İki, and M. Arslan, "Investigation on improvement in shear performance of reinforced-concrete beams produced with recycled steel wires from waste tires," *Sustainability*, vol. 14, no. 20, p. 13360, September 2022. [Online]. Available: <https://doi.org/10.3390/su142013360>
- [20] S. Qaidi, H. Najm, S. Abed, Y. Ozkılıç, H. A. Dughaisi, M. Alost, M. Sabri, F. Alkhatib, and A. Milad, "Concrete containing waste glass as an environmentally friendly aggregate: a review on fresh and mechanical characteristics," *Mater.*, vol. 15, no. 18, p. 6222, 2022. [Online]. Available: <https://doi.org/10.3390/ma15186222>
- [21] I. Agwa, A. Zeyad, B. Tayeh, and M. Amin, "Effect of different burning degrees of sugarcane leaf ash on the properties of ultrahigh-strength concrete," *J. Build. Eng.*, vol. 56, no. 8, p. 104773, 2022. [Online]. Available: <http://doi.org/10.1016/j.jobte.2022.104773>
- [22] I. S. Agwa, A. Zeyad, B. Tayeh, A. Adesina, A. de Azevedo, M. Amin, and M. Hadzima-Nyarko, "A comprehensive review on the use of sugarcane bagasse ash as a supplementary cementitious material to produce eco-friendly concretes," *Mater. Today: Proc.*, vol. 55, no. 1, p. 688–696, 2022. [Online]. Available: <http://doi.org/10.1016/j.matpr.2022.03.264>
- [23] J. A. Neto, M. de França, and D. R. N. Sd Amorim Júnior, "Effects of adding sugarcane bagasse ash on the properties and durability of concrete," *Constr. Build. Mater.*, vol. 266, no. part A, p. 120959, 2021. [Online]. Available: <https://doi.org/10.1016/j.conbuildmat.2020.120959>
- [24] S. Minnu, A. Bahurudeen, and G. Athira, "Comparison of sugarcane bagasse ash with fly ash and slag: An approach towards industrial acceptance of sugar industry waste in cleaner production of cement," *J. Cleaner Prod.*, vol. 285, no. 401595, p. 124836, 2020. [Online]. Available: <http://doi.org/10.1016/j.jclepro.2020.124836>
- [25] V. Katara and M. Madurwar, "Pozzolanic performance resemblance of milled sugarcane biomass ash using different pozzolanicity test methods," *Advances in Cement Research*, vol. 32, no. 5, p. 205–215, 2020. [Online]. Available: <https://doi.org/10.1680/jadcr.18.00061>
- [26] L. C. de A. Mello, M. dos Anjos, M. de S a, N. de Souza, and E. de Farias, "Effect of high temperatures on self-compacting concrete with high levels of sugarcane bagasse ash and metakaolin," *Construction and Building Materials*, vol. 248, no. 5, p. 118715, 2020. [Online]. Available: <http://doi.org/10.1016/j.conbuildmat.2020.118715>
- [27] S. Sebastin, A. Priya, A. Karthick, R. Sathyamurthy, and A. Ghosh, "Agro waste sugarcane bagasse as a cementitious material for reactive powder concrete," *Clean Technol.*, vol. 2, no. 4, p. 476–491, 2020. [Online]. Available: <http://doi.org/10.3390/cleantechnol2040030>
- [28] B. Ribeiro, T. Uchiyama, J. Tomiyama, T. Yamamoto, and Y. Yamashiki, "Development of interlocking concrete blocks with added sugarcane residues," *Fibers*, vol. 8, no. 10, p. 61, 2020. [Online]. Available: <https://doi.org/10.3390/fib8100061>
- [29] I. Hakeem, I. Agwa, B. Tayeh, and M. Abd-Elrahman, "Effect of using a combination of rice husk and olive waste ashes on high-strength concrete properties," *Case Studies in Construction Materials*, vol. 17, no. 3, p. e01486, 2022. [Online]. Available: <https://doi.org/10.1016/j.cscm.2022.e01486>
- [30] I. Hakeem, M. Amin, A. Zeyad, B. Tayeh, A. Maglad, and I. Agwa, "Effects of nano sized sesame stalk and rice straw ashes on high-strength concrete properties," *J. Clean. Prod.*, vol. 370, no. 7, p. 133542, 2022. [Online]. Available: <http://doi.org/10.1016/j.jclepro.2022.133542>
- [31] M. A. Sherif, B. Tayeh, M. Kandil, I. Agwa, and M. Abdelmagied, "Effect of rice straw ash and palm leaf ash on the properties of ultrahigh-performance concrete," *Case Stud. Constr. Mater.*, vol. 17, no. 5, p. e01266, 2022. [Online]. Available: <http://doi.org/10.1016/j.cscm.2022.e01266>
- [32] R. Velmurugan, G. Balaganesan, N. Kakur, and K. Kanny, *Dynamic Behavior of Soft and Hard Materials Volume 1: Proceedings of 13th International Symposium on Plasticity and Impact Mechanics 2022*, ser. Springer Proceedings in Materials. Springer Nature Singapore, 2023. [Online]. Available: <https://books.google.iq/books?id=NbjrEAAQBAJ>
- [33] S. K. Nambiar and et al., "Indian standard methods of test for aggregate for concrete," *Bureau of Indian Standards, New Delhi*, vol. IS:2386, no. Part I, 1963. [Online]. Available: <https://law.resource.org/pub/in/bis/S03/is.2386.1.1963.pdf>
- [34] V. Katara and M. Madurwar, "Specification for silica fume," *Adv. Cem. Res.*, vol. IS 15388, 2003.
- [35] B. Standard, "Fibres for concrete-part 2: Polymer fibres-definitions, specifications and conformity," *The European Standard EN 14889-2:2006 has the status of a British Standard*, 2006.
- [36] I. Standard, "Plain and reinforced concrete-code of practice," *Bureau pf Indian Standards*, vol. IS456, no. 2000, 2007.
- [37] H. Zhang, T. Ji, X. Zeng, Z. Yang, X. Lin, and Y. Liang, "Mechanical behavior of ultra-high performance concrete (uhpc) using recycled fine aggregate cured under different conditions and the mechanism based on integrated microstructural parameters," *Construction and Building Materials*, vol. 192, pp. 489–507, 2018. [Online]. Available: <https://doi.org/10.1016/j.conbuildmat.2018.10.117>
- [38] A. C. 1437-07, "Standard test method for flow of hydraulic cement mortar," *ASTM*, vol. 32, no. 5, 2009.
- [39] ASTM, "Standard practice for fabricating and testing specimens of ultra-high performance concrete," *ASTM C1856/C1856M 17*, vol. 32, 2020.
- [40] I. Standards, "Indian standard methods of test for strength of concrete. bureau of indian standards, new delhi," *SHRI E. A. NADIRSHAH and El At.*, vol. IS: 516, no. 1959., 2020.
- [41] ASTM, "Standard test method for static modulus of elasticity and poisson's ratio of concrete in compression," *ASTM C 469-02*, 2021.
- [42] B. E. 12390-8, "Testing hardened concrete part 8: Depth of penetration of water under pressure," *BSI*, 2009.
- [43] K. H., H. F., and B. M. T., "Masonry mortar with nanoparticles at a low temperature," *Proceedings of the Institution of Civil Engineers: Construction Materials*, vol. 110, no. 6, pp. 297–308, 2017. [Online]. Available: <https://doi.org/10.1680/jcoma.15.00054>
- [44] K. A. S., N. H., Y. A. A., M. S., and R. M. T. M., "The effects of nanoparticles of silica and alumina on flow ability and compressive strength of cementitious composites," *Key Engineering Materials*, vol. 631, no. 5, p. 119–127, 2014. [Online]. Available: <https://doi.org/10.4028/www.scientific.net/KEM.631.119>
- [45] N. A., and R. S., "Improvement compressive strength of concrete in different curing media by al2o3 nanoparticles," *Materials Science and Engineering*, vol. 528, no. 3, p. 1183–1191, 2011a. [Online]. Available: <https://doi.org/10.1016/j.msea.2010.09.098>
- [46] N. A., and R. S., "Al2o3 nanoparticles in concrete and different curing media," *Energy and Buildings*, Elsevier, vol. 43, no. 6, pp. 1480–1488, 2011b. [Online]. Available: <http://doi.org/10.1016/j.enbuild.2011.02.018>
- [47] ASTM-C109/C109M-07, "Compressive strength of hydraulic cement mortars (using 2-in . or 950-mm0 cube specimens)," *ASTM*, 2020.
- [48] A. M. R., J. M. R., and M. E., "To study the effect of adding al2o3 nanoparticles on the mechanical properties and microstructure of cement mortar," *Life Science Journal*, vol. 8, no. 4, p. 613–617, 2011.
- [49] A. C1723, "Standard guide for examination of hardened concrete using scanning electron microscopy," *ASTM*, 2016.

How to cite this article:

S. Hariprasad Reddy, K Mahaboob Peera, A. Surendra, Cholker Arvind kumar and Meruva Leelakar, (2025). 'Role of nano-Al2O3 in modifying the properties of ultra-high-performance concrete', Al-Qadisiyah Journal for Engineering Sciences, 18(1), pp. 72-77. <https://doi.org/10.30772/qjes.2024.153324.1376>